Modeling Physical Information of Molecular Wires Using Conductance Histograms

Patrick Williams

June 21, 2013

1 Introduction

The exploration into electron transport of molecular systems has become an active topic in the world of quantum physics and electronics [4]. This research heavily affects the future development of new technologies such as photovoltaic, thermo-electrics, and molecular electronics, and raises fundamental questions into the differences in conventional electronics versus quantum electronics. Compared to conventional electronics in which there are no channels, molecular systems have a finite number of channels through which the electrons can travel and maximum limits to the conductance in the channel [2] [5]. These channels are analogous to a city layout, where traveling through a city can involve many unique paths using different streets and directions. Each combination of paths would be similar to a single channel within these quantum systems.

Within each channel, there is a probability that describes how likely it is that an electron will travel from one electrode to the other. If a channel is closed, it is said to have a conductance of zero and if the channel is open, the conductance is one; meaning if an electron enters the channel, it has a 100 percent probability of traveling across the electrodes [5]. However, each channel is not limited to an open or closed state, but rather a spectrum

of conductances that do not ensure a 100 percent probability of electron transport. Most of the molecular systems have average conductance values that are not completely open or closed states, meaning that the electron has a certain probability of making it from one electrode to the other. Molecular systems are made up of both the individual channels and the physical details that affect the conductances of the systems, such as Γ, ϵ, and E_F. The physical details that affect the conductances, g, of the molecular systems are: the coupling strength of the molecular conductor, Γ, the Fermi Energy of the electrodes, E_F, and the energy of the conductor, ϵ. The purpose of this research is to better understand how these three physical details of the molecular system affect the measured conductance.

Currently, when scientists run experiments on these nano-scale conductors, it is not known how to hold the physical details constant in order to evaluate the outcomes of these tests. Between each test, the way the molecule channel couples to the electrode varies making the tests irreproducible and difficult to analyze, raising the question of how to measure the physical aspects that, to date, cannot be controlled [3]. Likewise, the properties that influence these channels and create optimal conductors are different to measure and hold constant. In order to solve the problems raised by this process, scientists order the outcomes in histograms, and have concluded that these conductances organize into single-channel peaks as seen in Figure 1 [3]. Within these histograms, the peak is said to be the system's single- molecule conductance.

Scientists currently know that the shape of these peaks holds information about the chemistry of the system, but little research into histogram analysis has been done. It is now possible to simulate these peaks using a given set of parameters, E_F, ϵ, Γ, and the method with which to predict the peak of the histogram, but better interpretation of the experimental parameters through analyzation of the peaks of the conductance histogram is needed. In order to extract the parameters that affect the conductance histogram, the model devised must be able to solve an inverse problem in which the total amount of data and outcomes are known, but the actual input values are unknown. Also, the model devised should be

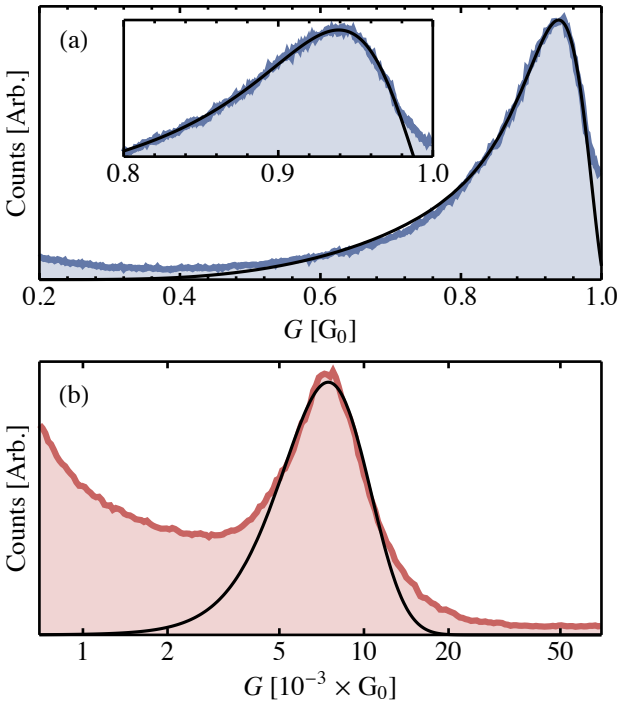

Figure 1: This conductance histogram is experimental data using a gold point contact. This histogram plots the times a conductance is measured versus actual conductance of the single channel. In case (a), the resonance fitter is used, and in case (b) the non-resonant tunneling fitter is used.

able to relate to physical data that affects the tests. Presently, analysis over the data or line shapes has not been done. The only analysis done has been over empirical models that were used to describe the data. This the model devised must be able to estimate what values and physical information are affecting the line shapes of single-channel peak histograms. Therefore the primary point of this research is to understand what fundamental physics is affecting the outcome of these conductances. If it is possible to understand these fundamental processes, then new, groundbreaking work can be done into fields dealing with quantum electron transport.

2 Background

2.1 Conductance Histograms

Conductance histograms are a useful tool when analyzing electron transport through molecular or quantum systems. However, the experimental measurements recorded from these systems vary significantly and need further analysis to interpret [3]. Results have proven the sensitivity of conductance to change in the molecule- electrode interface [3]. In each experimental histogram, the x-axis is the measured conductance and the y-axis is number of times observed , or approximately the probability of observation as seen in Figure 1.

Even though much progress has been made into understanding single channel conductance, it is hard to determine all the properties that affect this process. Therefore, in past experiments scientists have had much difficulty determining the microscopic details, such as coupling strength and channel's energy, surrounding the molecule-electrode interfaces, or even control them.

Additionally, the width of this peak is attributed to the chemistry and structure of the molecule and how it conducts these electrodes. Depending on the geometry of the molecule, such as packing angles, the conductance can vary greatly [3]. The geometry of the molecule can determine the path by which the electron travels to the opposite electrode. The more possible paths an electron can take, the wider the variance, or deviation, of the histogram. In this work, the line shapes of the peaks of the conductance histograms are explored because of the information pertaining to the physical details that could be contained in the line's shapes [3]. Primarily, from this peak two cases of electron transport mechanism, either resonant or non-resonant tunneling, can be found. All of this information in these systems is then quantized, meaning that there is a specific number of channels by which the electrons can flow through the system [5]. Each one of these channels has a well-defined probability that an electron can successfully make it from one electrode to another [5][2]. The total (zero-bias)

conductance, conductance without any confounding variables, is given by

$$G = G_0 T(E_F) \tag{1}$$

where $T(E_F)$ is the total of all transmission probabilities through all channels, E_F is the Fermi Energy [2]. G_0, the quantum of conductance, is then calculated by:

$$(G_0) = \frac{2e^2}{h} \tag{2}$$

where e is the electron charge, and h is Planck's constant [5][2]. The conductance is viewed as the probability that the electron will make it across the system to the electrodes, and subsequently is equal to transmission [**?**]. The conductance through any channel is limited to $0 \leq G \leq G_o$ [5].

Recently, there has been new research into the single channel peaks of the histograms because its additional relevant data can still be extracted [3]. These peaks not only show what is referred to as the "expected conductance" through a system, but also the conduction mechanism (resonant vs. non resonant tunneling) [5]. This line shape formed by the histogram also relates to the probability density function (PDF) for measuring the conductance through system and the line shape of a one-channel peak can be described and modeled by a "double beta" distribution, log-normal distribution, normal distribution, and Lorentzian distributions, but these fitting parameters have no physical significance to the system [1][5].

2.2 Landauer-Imry Theory

In the Landauer- Imry theory, transmission in these quantum systems can be viewed as conductance. Landauer and Imry developed Equation 1. In this transmission function, three primary details affect the transmission, as seen in Figure 2:

1. The coupling site energy to the left and right electrode, called Γ_L and Γ_R respectively.

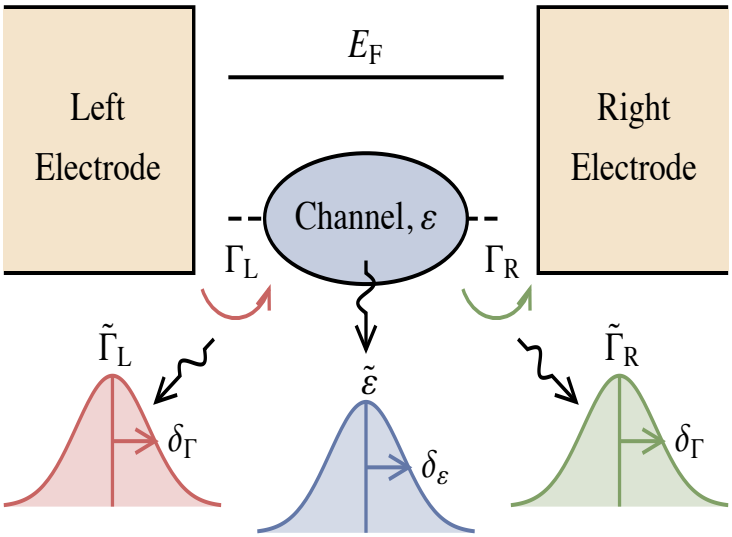

Figure 2: In the schematic, the conductor forms a channel while sandwiched between two electrodes. In order to simulate experimental uncertainty within the model, each physical detail is assumed to be an independent variable that can be described by a mean and standard deviation. In this case $\tilde{\Gamma_L}$ is the mean value of the left coupling site and has a standard deviation of δ_L.

2. The Fermi Energy of the electrodes is E_F.

3. The energy of the channel, ϵ.

In the cases evaluated, it is assumed that $\Gamma_L \geq 0$ and $\Gamma_R \geq 0$. Therefore, the transmission, $T(E)$ would be [2],

$$T(E) = \frac{4\Gamma_L\Gamma_R}{4(E_F - \epsilon)^2 + (\Gamma_L + \Gamma_R)^2} \tag{3}$$

The purpose of modeling the conductance histograms is to see how these variables will affect the system. If these variables can be measured and understood, then a better evaluation of the molecular systems can be developed. A single- channel system with two electrodes, in the broadest case requires Γ_L, Γ_R, and ϵ to model the electron transport [5]. If ($E_F \approx \epsilon$) then the transport is "resonant" as seen in case 1 of Figure 3. If the Fermi Energy and Epsilon are not roughly equivalent to each other, then the test is considered to be "non-resonant," as seen in cases 2 and 3.

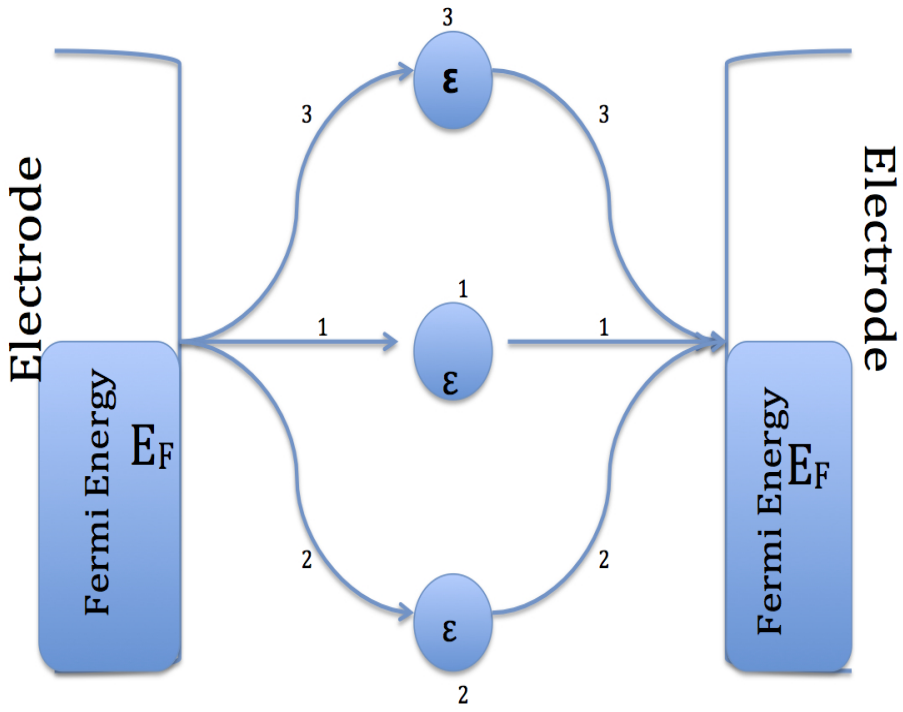

Figure 3: This figure shows the interaction of the Fermi Energy with the energy level, ϵ, of the molecule or atom creating the channel. Path 1 is considered to be resonant and paths 2 and 3 are non- resonant.

2.3 Resonant Tunneling

In the resonant tunneling case for electron transport, the electron enters the system when the energy of the molecule energy (ϵ) equals the Fermi Energy of the electrode. The Fermi Energy or energy is the electron occupation on the two electrodes as seen in Figure 3, case 1. The lower the Fermi Energy of an electrode, the fewer electrons occupy the electrodes in any state. With resonant tunneling, the electron has a much higher chance of making it through the channel. The channel is considered to be open when it is at resonance. When the channel is open, the measured conductance will be the greatest and equal to the quantum of conductance, as seen in Equation 2 [5].

2.4 Non-resonant Tunneling

In the non-resonant case, the energy of the molecular channel is off the Fermi Energy of the electrode, meaning that the $\epsilon \neq E_F$. In Figure 3, cases 2 and 3 are both non-resonant cases. In case 3, the energy of the conductor is above the Fermi Energy. In case 2, the conductor's energy is less than the Fermi Energy of the electrode, and in both cases there is more scattering of the electrons. Because of the increased probability for scattering, the conductance values measured will be less than the resonant case. Also, the conductance measured in the non-resonant case will not be the same as the quantum of conductance as in resonant tunneling. The channels are considered not open, and will have a much lower measured conductance compared to the resonant case.

3 Methods

In order to evaluate conductance histograms and the cases (resonance versus non-resonance), first a model was made using probability theory which gave the integral in equation 4 [1]. This integral was then evaluated and simplified, and fitting parameters for the model were extracted for the different resonant and non-resonant cases as seen by the c and d values in

Equations 5 and 6. This model was then validated and applied to experimental data. This model will be able to extract important details and information from the line shapes of these conductance histograms. The integral given by probability theory is,

$$\hat{G}(g) = \int_{-\infty}^{\infty} d\epsilon \int_{0}^{\infty} d\Gamma \hat{P}_{\epsilon} \hat{P}_{\Gamma}(\Gamma) \delta \left(\frac{\Gamma^2}{(E_F - \epsilon)^2 + \Gamma^2} - g \right) \tag{4}$$

When this integral was evaluated it was found that, in the end, the probability density function only has one free parameter, $c \equiv \frac{\Gamma_0}{\delta_\epsilon}$. Therefore the final equation after evaluation for the at resonance case is,

$$\hat{G}(g) \approx \frac{1}{\sqrt{2\pi g^3 (1-g)}} c \exp\left(-c^2 \frac{1-g}{2g} \right) \tag{5}$$

Equation 5 is used to create the control histograms.

In the non-resonance case, the statistical integral is evaluated to be,

$$\hat{G}(g) = \frac{c}{\sqrt{8\pi g (1-g)^3}} \exp - \frac{(c\sqrt{g} - d\sqrt{1-g})^2}{2(1-g)} \tag{6}$$

and in this case there are two free parameters, $c \equiv \frac{|E_F - \epsilon|}{\delta_\Gamma}$ and $d \equiv \frac{\Gamma_0}{\delta_\Gamma}$. These two parameters will be used when evaluating the histograms.

3.1 Validation

To validate the equations used to model the histograms, a control experiment must be devised. First a program was written in C++ that simulated control points when given the input values of $\Gamma_L, \Gamma_R, \epsilon$, and E_F. These "data points" were actually certain $\Gamma_L, \Gamma_R, \epsilon$, and E_F with their deviations and the different conductances measured for those $\Gamma_L, \Gamma_R, \epsilon$, and E_F values. The program had to use a random number generator in order to simulate the experimental uncertainty, as seen in Figure 4 step 1. This program simulated several hundred data points, and this data was then sent to a binning program that organized the

simulated data points into a conductance histogram in which the input values were known. From here, the fitting program written was fitted to the histogram. In Figure 4, the python script was written in order to streamline the whole process of testing hundreds of conductance histograms.

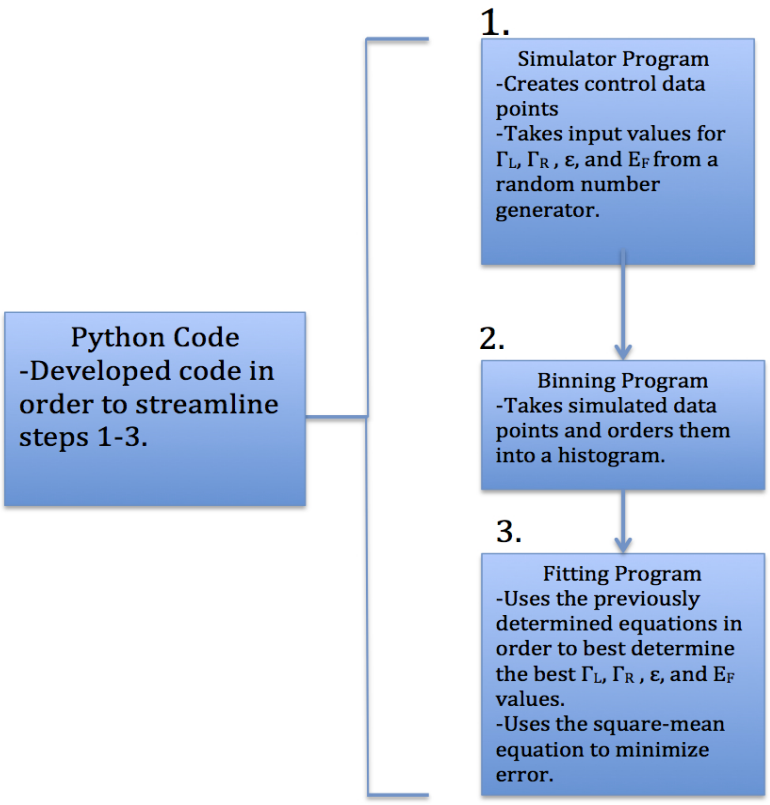

Figure 4: the chart shows the control experiment set up used to validate the fitting program. The python script was used to streamline the process over hundreds of tests.

This program used Equations 5 and 6 for the different scenarios in which the simulated data could be at resonance or off-resonance. The fitting program used the root mean square equation,

$$\sum_i (P_i - P(g_i, c))^2 \tag{7}$$

to minimize the the difference between the input values P_i and the fitting function $P(g_i, c)$,

with parameters c. When Equation 6 was minimized, the output mean values of the parameters were measured.

4 Application

After the fitting program was validated, it has been applied to experimental data. So far the fitting has proven to be accurate and provided much insight into the way the two couplings Γ_L and Γ_R react in the system.

5 Results and Discussion

After running the evaluation program, it was concluded that the this fitting program is feasible. After getting the results from the validation, the input values for Γ, ϵ, and E_F were plotted against the output values for the fitting program as seen in Figure 5.

5.1 Resonant Fitter

In Figure 5, case (a) is the symmetric model with fitting parameter c. The fitting program is able to predict the values accurately. Therefore the symmetric fitter is reliable. Case (b), this is the asymmetric case with parameter c, when $\Gamma_L \neq \Gamma_R$. This case breaks down when $\Gamma_R \approx \Gamma_L$, as indicated by the red dots. This fitter breaks down because the values are starting to approach the symmetric case and therefore the asymmetric fitter cannot perform as well. Case (c) is the asymmetric fitter finding Γ_L, and it is accurate except when fitting close to the symmetric case. Case (d) is the same as case (c) except (d) plots the Γ_R. In order to explore what was happening at these red- dot cases in (b), (c), and (d) these histograms were examined in cases (e), (f), and (h). In each case, the fitting function is represented by the blue line and the model fit is represented by the red line. In each histogram, both the blue and red line match up, but the Γ values are tough to determine because it is so near

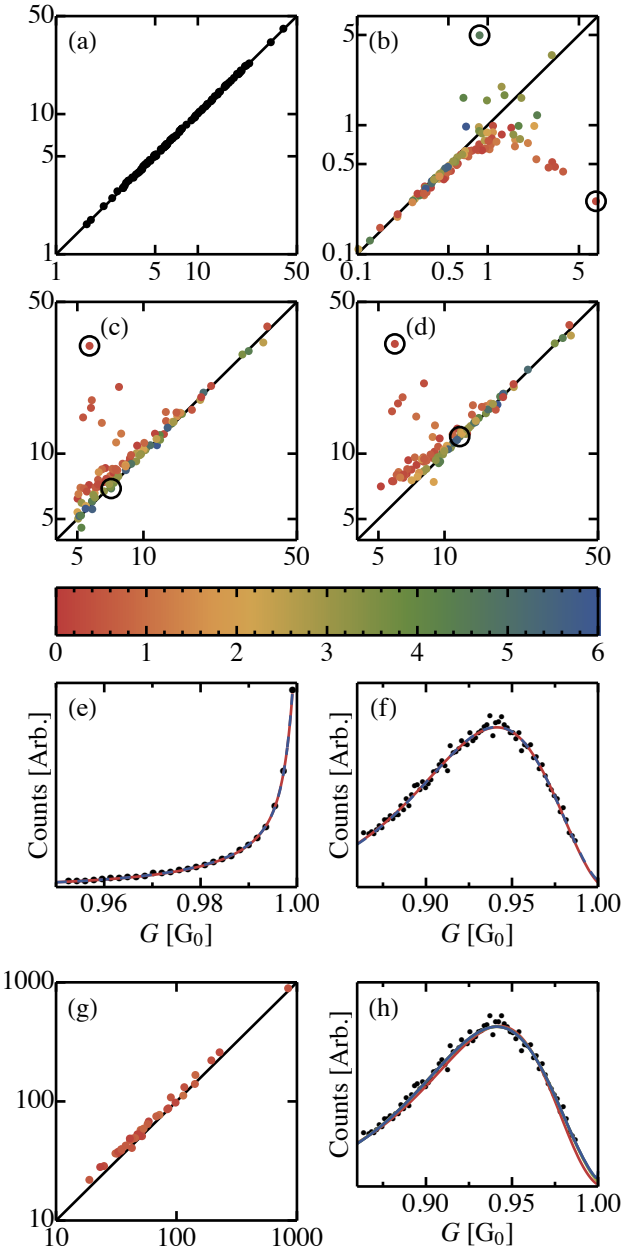

Figure 5: This is the resonant case histograms with the plotted values taken from the fitting program plotted against the actual input values. (a) Fit value of γ vs. the input value of γ for 100 simulated histograms. (b), (c), and (d) are similar plots as in panel (a) for the r, γ_L, and γ_r respectively. (e) Is the histogram for the red circled point in panels (b)-(d). The red line is the predicted line shape from the input parameters and the blue line is the best- fit line shape. (f) is the histogram for the green circled point in panels (b)-(d). (g) is a similar plot as in panels (b)-(d) but for the value of r, γ_L, and γ_R when $\mid \gamma_L - \gamma_R \mid \approx 0$. (h) is the best- fits to the histogram in panel (f) with r fixed to values between 0.5 and 10. The shading in this figure represents $\mid \Gamma_L - \Gamma_R \mid$

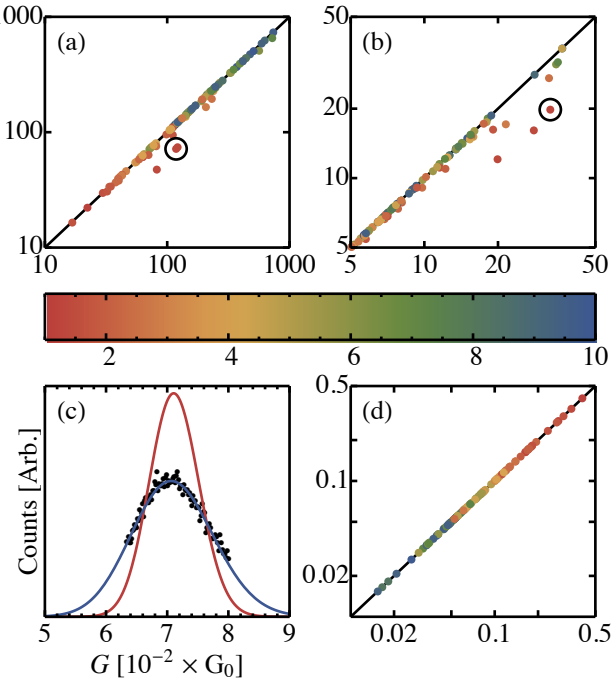

Figure 6: This is the non- resonant case histograms with the plotted values taken from the fitting program plotted against the actual input values. (a) is the fit value of c vs. the input value of c for 100 simulated histograms. (b) is similar to the (a) panel except for using the parameter d using the same histograms. (c) is the histogram for the circled data points in panels (a) and (b). The red line is the predicted line shape from the parameters input to the simulator ($c = 118$ and $d = 32.7$). The blue line is the best- fit line shape ($c = 71.7$ and $d = 19.8$). In this case, the values of g are too large to justify $g \ll 1 - g$ and the model is invalid. (d) similarly plots the value of d/c as in panel (a) and (b). The shading in this figure represents $\mid E_F - \epsilon_0 \mid \gg 0$.

the symmetric case. Also the green dots are cases in which the E_F and ϵ values start to approach the non-resonant case, so the fitter begins to fail. Here it would probably be best to apply the non- resonant fitter. The fitter written is reliable, but if the conditions start to approach another type of model then the fitter begins to break down.

5.2 Non-resonant Fitter

In Figure 6, case (a) is the c parameter extracted out of the non-resonant model. Case (b) shows how the parameter d was accurate in the evaluations. All of the inefficient fits are red in color because in the derivation of the model it was assumed that $\mid E_F - \epsilon_0 \mid \gg 0$ and in

these cases this difference between E_F and ϵ was not great enough. Thus in these cases, the derived model begins to break down. Case (c) shows how the red line (input parameters) are not matching with data, but the fitting program is working. In this case the model is less effective because the derivations made false assumptions. In case (d), it is interesting to note though that parameters $\frac{d}{c}$ which means the parameters are working.

5.3 Experimental Data

After receiving data from Professor Latha Venkataraman of Columbia, the fitting program was used on the data. In Figure 1, the top graph (a) is a gold-point contact (resonant). The values extracted were that $\Gamma_1 = 7.43$ and $\Gamma_R = 11.5$ and $c = 0.281$. Interestingly enough, the right coupling seems to be about 150% greater than the left. This is the first time this information has been know to the scientific community. In the bottom graph (b), benzenediamine (non-resonant) was used as the conductor. In this case the values extracted were $c = 64.7$ and $d = 5.79$. The initial hill at the beginning of this graph is background signal from the vacuum tunneling. This fitting program has already proved valuable in determining actual values from experimental data.

6 Conclusion

In summary, the goal of the project was to create a better tool for analyzing conductance histograms. A model was determined from heavy statistical analysis of probability theory, and an equation was used to model these histograms using the fitting parameters c and d . After the fitting program was validated, it was applied to experimental data. In this analysis, more was learned about the way that the conductors couple with electrodes. This work has never been done, and the model can be applied to future research into the area of quantum conductances where it will be valuable and useful when understanding the physical details motivating quantum conductances. This research can be then used in ground-breaking areas

such as thermo-electrics, photo-voltaics, and molecular electronics.

References

[1] S. Ghahramani. *Fundamentals of Probabilty.* Prentice- Hall, Upper Saddle River, NJ, USA, 2nd edition, 2000.

[2] Rolf Landauer; Yoseph Imry. Conductance viewed as transmission. *Reviews of Modern Physics*, 71(2):306–312, 1999.

[3] Matthew G Reuter, Mark C Hersam, Tamar Seideman, and Mark A Ratner. Signatures of cooperative effects and transport mechanisms in conductance histograms. *Nano Lett*, 12(5):2243–8, May 2012.

[4] J.C. Cuevas; E. Sheer. *Molecular Electronics.* World Scientific, 2010.

[5] Matthew G. Reuter; Patrick D. Williams. Extracting physical information from the line shapes of single- channel peaks in conductance histograms. 2012.